

Towards near-permanent CoCrMo prosthesis surface by combining micro-texturing and low temperature plasma carburising

Dong, Yangchun; Svoboda, Petr; Vrbka, Martin; Kostal, David; Urban, Filip; Cizek, Jan; Roupцова, Pavla; Dong, Hanshan; Krupka, Ivan; Hartl, Martin

DOI:

[10.1016/j.jmbbm.2015.10.023](https://doi.org/10.1016/j.jmbbm.2015.10.023)

License:

Creative Commons: Attribution-NonCommercial-NoDerivs (CC BY-NC-ND)

Document Version

Peer reviewed version

Citation for published version (Harvard):

Dong, Y, Svoboda, P, Vrbka, M, Kostal, D, Urban, F, Cizek, J, Roupцова, P, Dong, H, Krupka, I & Hartl, M 2016, 'Towards near-permanent CoCrMo prosthesis surface by combining micro-texturing and low temperature plasma carburising', *Journal of the Mechanical Behavior of Biomedical Materials*, vol. 55, pp. 215-227. <https://doi.org/10.1016/j.jmbbm.2015.10.023>

[Link to publication on Research at Birmingham portal](#)

Publisher Rights Statement:

After an embargo period this document is subject to the terms of a Creative Commons Attribution Non-Commercial No Derivatives license

Checked Feb 2016

General rights

Unless a licence is specified above, all rights (including copyright and moral rights) in this document are retained by the authors and/or the copyright holders. The express permission of the copyright holder must be obtained for any use of this material other than for purposes permitted by law.

- Users may freely distribute the URL that is used to identify this publication.
- Users may download and/or print one copy of the publication from the University of Birmingham research portal for the purpose of private study or non-commercial research.
- User may use extracts from the document in line with the concept of 'fair dealing' under the Copyright, Designs and Patents Act 1988 (?)
- Users may not further distribute the material nor use it for the purposes of commercial gain.

Where a licence is displayed above, please note the terms and conditions of the licence govern your use of this document.

When citing, please reference the published version.

Take down policy

While the University of Birmingham exercises care and attention in making items available there are rare occasions when an item has been uploaded in error or has been deemed to be commercially or otherwise sensitive.

If you believe that this is the case for this document, please contact UBIRA@lists.bham.ac.uk providing details and we will remove access to the work immediately and investigate.

Author's Accepted Manuscript

Towards near-permanent CoCrMo prosthesis surface by combining micro-texturing and low temperature plasma carburising

Yangchun Dong, Petr Svoboda, Martin Vrbka, David Kostal, Filip Urban, Jan Cizek, Pavla Roupцова, Hanshan Dong, Ivan Krupka, Martin Hartl



PII: S1751-6161(15)00396-3
DOI: <http://dx.doi.org/10.1016/j.jmbbm.2015.10.023>
Reference: JMBBM1664

To appear in: *Journal of the Mechanical Behavior of Biomedical Materials*

Received date: 21 July 2015
Revised date: 28 September 2015
Accepted date: 23 October 2015

Cite this article as: Yangchun Dong, Petr Svoboda, Martin Vrbka, David Kostal, Filip Urban, Jan Cizek, Pavla Roupцова, Hanshan Dong, Ivan Krupka and Martin Hartl, Towards near-permanent CoCrMo prosthesis surface by combining micro-texturing and low temperature plasma carburising, *Journal of the Mechanical Behavior of Biomedical Materials*, <http://dx.doi.org/10.1016/j.jmbbm.2015.10.023>

This is a PDF file of an unedited manuscript that has been accepted for publication. As a service to our customers we are providing this early version of the manuscript. The manuscript will undergo copyediting, typesetting, and a review of the resulting galley proof before it is published in its final citable form. Please note that during the production process errors may be discovered which could affect the content, and all legal disclaimers that apply to the journal pertain.

Towards near-permanent CoCrMo prosthesis surface by combining micro-texturing and low temperature plasma carburising

Yangchun Dong 1,2*, Petr Svoboda 1, Martin Vrbka 1, David Kostal 1, Filip Urban 1, Jan Cizek 3, Pavla Roupcova 2, Hanshan Dong 4, Ivan Krupka 1, Martin Hartl 1

1. Faculty of mechanical engineering, Brno university of technology, Brno, 616 69, Czech Republic

2. Central European Institute of Technology (CEITEC), Brno, 602 00, Czech Republic

3. NETME Centre, Institute of Materials Science and Engineering, Brno University of Technology, 616 69, Czech Republic

4. School of Metallurgy and Materials, Birmingham University, B15 2TT UK

*E-mail: yangchun.dg@gmail.com

Abstract

An advanced surface engineering process combining micro-texture with plasma carburising process was produced on CoCrMo femoral head, and their tribological properties were evaluated by the cutting-edge pendulum hip joint simulator coupled with thin film colorimetric interferometry. FESEM and GDOES showed that precipitation-free C S-phase with uniform case depth of 10 μm was formed across the micro-textures after duplex treatment. Hip simulator tests showed that the friction coefficient was reduced by 20 % for micro-meter sized texture, and the long-term tribological property of micro texture was enhanced by the C-supersaturated crystalline microstructure formed on the surface of duplex treated CoCrMo, and thus was significantly enhanced biotribological durability. In-situ colorimetric interferometry confirmed that the maximum film thickness around texture area was 530 nm, indicating that the additional lubricant during sliding motion might provide exceptional bearing life.

Highlights:

- An innovative duplex surface treatment (micro-texturing and S-phase) was developed.
- In-situ visualization of lubricating films on real geometry head and cup.
- Lubricating film thickness was increased by surface texturing on CoCrMo head.
- Testing time-dependant performance of dimpled surface and its longevity.

- Study of frictional behaviour of MoP joints with different texture geometries.

Keywords: plasma carburising, surface texturing, wear, biotribology, colorimetric interferometry, friction

1 Introduction

Hip arthroplasty surgery is considered a successful intervention to restore hip functionality and relief pain to patients with severe joint disease or trauma. Surface engineering of materials used within prosthesis is presented as possible measure to prevent aseptic loosening and surgical site infections due to the shedding of prosthesis materials from fretting and tribocorrosion. Volumetric wear determined by the hip simulator test showed that UHMWPE MoP hip prostheses exhibited great wear rate of 40-80mm³/million-cycles, and cross-linked MoP exhibited 5-40 mm³/million-cycles. For other types of hip prostheses, the wear rate was in the range of 0.01-1.2 mm³/million-cycles [1-4]. The dissemination of wear particles to liver, spleen or lymph nodes after hip arthroplasty is a common feature regardless of what type of bearings used [3]. This showed that even for MoP bearings a certain amount of metallic debris particles can be disseminated in the body. Metal particles with size of 10-100 nm are highly mobile. It may be internalised by cells even though a small mass fraction is released. Clinical evidence showed that the metal iron produced around MoP bearings prosthesis may cause metal hypersensitivity or even pathologically cytotoxicity to macrophages. Chromosomal changes in bone marrow cells have been observed clinically with the presence of metal concentration on MoP metal implants [4].

A research by Ito et al. in 1990s concaved patterns on prosthesis hip replacement CoCr femoral head by electrical discharge etching method [5]. They observed remarkable 69 % less amount of wear on UHMWPE by introducing 0.1 mm deep dimples all around CoCr femoral head. Indeed, surface texturing (ST) is effective in control the amount of lubricant on the boundary lubricated bearing surfaces. Surface texturing has been introducing to general mechanics such as cylinder liner of internal combustion engines and planar thrust bearings [6]. Optimised texture patterns applied in cylinder liner can save up to

10 % mechanical losses and subsequently save 1.2-2.5 % fuel and energy. A few attempts to improve the biotribology of artificial joints by using surface texturing were reported [7-10]. Sawano et al. [8] tested four groups of CoCr heads with different dimpled depths rotation against UHMWPE and pointed out for the first time that dimples can indeed improve live of artificial joints. Choudhury et al. [11] observed the reduced third-body wear by creating CNC micro-drilling Ta-C DLC coating on femoral head. In the USA, Raeymaekers et al. [7] used laser patterned microtexture to increase the load-carrying capacity and reduce friction of the CoCr femoral head for MoP joints. Zhang and Wang et al. [10, 12] in China used metal-on-polymer disc wear tester to compare the friction coefficient of textured and untextured UHMWPE under various sliding speed and load. They found that optimum parameters cut friction coefficient by as much as 66.7–85.7 % and average reduction of wear is 35 %. Recently, Krupa et al. observed the effects of surface topography on lubrication film formation [13, 14]. It has been shown that the surface topography plays an important role during transient operational conditions and properly designed surface topography could help to increase the lubrication efficiency. It is worth noting that the friction coefficient is variable with the textured materials and the range of sliding speed, and geometric parameters. Among them, analysis on the effect of geometric parameters of dimples is considered high priority to mitigated the risk of no benefit or even adverse effect to the wear of MoP bearings [8].

Nevertheless, Hsu et al. [15] noticed texture can reduce the friction initially but soon it becomes a little rough even at lowest pressure. Hsu suggested that chemistry modification or coatings to protect the textures need to be developed. Krupka and Vrbka et al. [13, 16-19] also reported that the degradation of indentation found after fatigue test indicated that the failure of component was possibly attributed to the wear of the textured surface. Therefore, improvement measures can be focused on to increase the surface durability of indentation served under high pressure conditions, which might assure adequate fatigue strength of patterned surface.

Plasma carburising (PC) process has been used to improve the wear and fatigue properties of many artificial joints materials and it offers many advantages over other coating and hardening processes, in

particular, better diffusion efficiency, low cost, reduced energy consumption, and the removal of significant environmental hazards [20, 21]. Recently, advanced plasma thermochemical treatment conducted at low temperature, i.e. LTPC, is being developed for CoCrMo alloys [22, 23] and for stainless steels [24]. Because the process is conducted at low temperature, mobility of substitutional elements is low thus precipitation can be prevented even at exceeded solubility. As a result, a layer of microstructure that is supersaturated with nitrogen namely 'S-phase' (short from Supersaturated Phase) or 'expanded austenite' was produced. S-phase is a very hard (800-1000 Hv) and wear resistant diffusion case thus high durability under load-bearing condition is experienced. Furthermore, S-phase layer has been extensively studied as a substrate for long-lasting hip prosthesis surfaces. Dong et al. [24-26] carried out systematic research work on low temperature plasma engineering of several types of biomaterial alloy, and found that the wear resistance could be increased by two orders of magnitude under dry sliding conditions.

To this date, there is little research on the time-dependant performance of dimpled surface and how the durability of dimpled material affects the biotribology of surfaces. This work aims to investigate the longevity of low friction properties by adding PC hardened case to the microtexture. The feasibility of using this method to achieve long-lasting low friction material surface for orthopaedic applications is also discussed.

2 Materials and methods

2.1 Material preparation and experiment procedures

Figure 1 shows the experimental flow chart and the illustrated cross-sectional treated surface at each stage of process. Branded total hip replacement joint CoCrMo Ø28/0 'M' Taper 12/14 femoral head (ISO 5832-12) and electron irradiated highly cross-linked UHMWPE cup (ISO 5834-1) were used for texturing and plasma carburising treatments. The femoral heads were textured with well-defined micro-dimples using two mechanical indenter machines, i.e. Rockwell roller indenter for fabricating texture on circumference of sample and Rockwell auto indenter for the tip of sample. A vertical movement and rotation of the roller

indenter were operated by step motors and a strain gauge was used to check the load. The LTPC process was conducted in a standard DC plasma furnace (Klöckner 40 kW, Germany) as described in [23], with gas mixture of 98.5 % H₂ and 1.5 % CH₄ and pressure of 4 mbar at 450 °C for 10 hours. Process parameters have been optimized by our previous studies [33]. Table 1 summarises the experiment parameters of the ST, the LTPC and the PC samples, as comparison to the untreated CoCrMo (UT). Three sizes of dimples controlled by indentation depth, i.e. $h=1.5\ \mu\text{m}$, $2.4\ \mu\text{m}$ and $9.5\ \mu\text{m}$, were created on femoral head with round shape (for $1.5\ \mu\text{m}$ and $2.4\ \mu\text{m}$) or pyramid shape (for $9.5\ \mu\text{m}$), and two texture patterns with different line shift (s) was create for $2.4\ \mu\text{m}$ sized samples. As shown in figure 2 by 3D optical profilometer, pattern ST2 and pattern ST3 was created with $s=40\ \mu\text{m}$ and $s=20\ \mu\text{m}$, respectively. The density of dimple's area is calculated in the last column of texture parameters.

2.2 Surface Characterisation

The treated CoCrMo heads were cross-sectioned, polished and electro-etched with DC source and 15 % HNO₃ solution. A field emission scanning electron microscope (FESEM, Oxford JEOL 7000) was used to examine the top surface morphology of texturing, and microstructure of cross-sectional PC treated samples. Elemental composition-depth profiling of the PC treated samples ($\varnothing 4\ \text{mm}$ detecting area) were measured using LECO GDS-750 QDP glow-discharge optical emission spectroscopy (GDOES). Minimum of three random locations on the treated surface were selected for analysis. The surface topography and roughness were measured at 3 random $0.314\times 0.235\ \text{mm}$ areas using non-contact 3D optical profilometer (Bruker Contour GT-X8). Surface roughness was given as centre line average (R_a). The phase constituents of alloyed surface were analysed using the SmartLab XRD (Rigaku, Japan) instrument with Cu K α ($\lambda=0.145\ \text{nm}$) radiation and fine focus lamp. X'Pert High Score software with the PCPDFWIN database was used to identify the presence of crystalline phases in the material surface. Mechanical properties of the treated surface were measured on CSM nano-indentation tester with load of 20 mN.

2.3 Friction coefficient tests

2.3.1 Pendulum simulation

Damping curve and friction coefficient of surfaces was obtained on the pendulum machine according to [27]. All femoral heads were finally polished with diamond paste as a standard procedure after the treatment. The contact pair of femoral head and acetabular cup was arranged in an inverted position with respect to anatomical position (figure 3). The metal head was fixed to the pendulum and the movement is controlled by pendulum arms carrying loads of an average human weight. A new UHMWPE taper liner was cemented in a sample pot of base frame using resin. The pendulum was rotated to place the femoral head at an initial offset angle of 16° with the cup, released, and allowed to oscillate freely in the flexion-extension plane with a frequency of 0.49 Hz.

In order to calculate a friction coefficient between contact components, a pendulum rotation was tracked using angular velocity sensor fixed to the pendulum and the oscillation data was then processed using MATLAB[®] software. The calculation of friction coefficient was based on linear decay of the pendulum rotation with time and cycle number according to Crisco et al. [27].

Lubricant used in this study was the BS solution (Sigma-Aldrich B9433, protein concentration 89.7 mg/ml) diluted with still water to a concentration of 25 % and a total protein content of 22.4 mg/ml; The lubricant was immediately stored in a 12 ml container and frozen at -20°C after preparation. All components, which were in the contact with BS were cleaned in 1 %w/w sodium dodecyl sulphate, rinsed in distilled water, and then washed in isopropyl alcohol ($\text{C}_3\text{H}_8\text{O}$) before assembly. It was defrosted one hour before measurements, and then was supplied to the acetabular cup prior to test. A vicinity of the contact pair was fully bathed during test, and the temperature of setup was maintained by the in-situ heating cartridges to the body temperature of 37°C .

A newly developed optical tester was used as a valuable experimental tool to evaluate the lubrication mechanism in the artificial joints [28]. A Cr-coated semi reflective glass cup was used to replace the

UHMWPE cup because the contact bodies must be optically transparent. This test method is modified from the conventional non-conformal chromatic interferograms but it is different in the way that this film thickness measurement was performed at the simulated plane-contact pressure of human joint (i.e. conformal contact). The chromatic interferograms were recorded with a high-speed complementary metal-oxide semiconductor (CMOS) digital camera and evaluated with thin film colorimetric interferometry. The sample showing lowest friction coefficient from pendulum CoF test were selected for the film thickness test and it was compared with the reference sample (UT). Interferograms at the start, the middle and the end of the test from each performed measurement were selected for future processing. Film thickness (u) with relation to the damping time (T) and the sliding speed (v) were analysed. Approximately 80 interferometry images in total were measured for each sample.

2.3.2 Reciprocating friction coefficient test

A pin-on-disc linear reciprocating tribometer (TE79, Phoenix-tribology, UK) was used to evaluate the dynamic friction coefficient of MoP bearing surface. Samples were subjected to the same processing (the same texture and carburising parameters) as above. A 3×3 mm UHMWPE pin was moving back and forth on flat CoCrMo surface under the pressure of 2.2 MPa. A self-aligning system was used to ensure full contact between pin and disc. The sliding stroke length of pin was 3 mm and the frequency was 1.12 Hz. The testing sample was bathed in diluted BS solution during test and 10-20 strokes was carried out to obtain the real-time changes of CoF between the textured CoCrMo and UHMWPE.

2.3.3 Long-term wear simulation

To further investigate the long-time friction properties of MoP hip joint, the untreated and duplex treated samples were subject to ball-in-cup sliding wear which was modified according to international standard ASTM G99 wear testing with pin-on-disc apparatus [29]. A UHMWPE acetabular liner (Ø28 mm) was rotating against the CoCrMo Ø28/0 femoral head at 66 rpm (0.031 m/s) which was fixed on a ball holder and loaded with 50 N. The treated femoral head was cleaned in isopropyl alcohol and assembled carefully

into the liners. Lubrication as described above was added to the cup prior to each test and the amount was monitored visually during test. After 16,560 cycles, femoral heads were retrieved from ball-in-cup machine. Friction coefficient was tested before and after wear on pendulum machine as illustrated in 2.3.1. This method was designed to measure the effect of wear to the CoF of joints after simulated long-term use of artificial joints. The mean friction coefficient was calculated from 6 times of repetitive tests for each sample.

3 Results

3.1 Material characterisation

3.1.1 Metallography and chemical composition

Both visual and SEM observations revealed that the top surface of CoCrMo femoral head was smooth after texturing (figure 4a). The centre line average roughness of R_a was 10 nm on the areas between textures. After the second step of low-temperature carburising treatments, a deposition layer composed by nano-particles was produced covering the surface and leading to increased roughness of 620 nm (figure 4b). The cross-section SEM reviewed that the duplex treated surfaces appeared three multi-layer structure: a top ultra-thin deposition layer (500 nm in thickness), and a 10 μm thick C S-phase featured modification case (figure 4c), followed by a 5 μm diffusion layer without clear interface with substrate. The modification case had likeness of the C S-phase morphology produced by DC plasma carburising on stainless steels [30], and it is worth noting that metallography of C S-phase showed high density of dislocations, slip lines, and deformation twins in the C S-phase layer as shown in figure 4c.

The elemental depth profiles of carbon after duplex treatment are illustrated in figure 4d. This profile showed a plateau type shape with a steep leading edge on the surface. It peaked at the outmost surface (6.5 wt%) and then decreased from the surface to the bulk. The depth profile of carbon by GDOES is in good agreement with the cross-sectional microstructure in figure 4c, suggested the total thickness of C S-

phase case including diffusion layer is around 15 μm . This ultra-high level of carbon concentration on the surface is the evidence of the para-equilibrium super-saturated atomic carbon associated with interstitial diffusion mechanism [22].

3.1.2 Crystallographic phases

The phase constitutions of treated and untreated CoCrMo heads are shown in figure 5. It can be seen that the untreated material is predominantly consisted of α -FCC and ϵ -HCP evidenced by intensities of α (111) and ϵ (101) peaks near 43.6° and 46.6° , respectively. This is similar to the microstructure of medical use dual phase CoCrMo alloy in the international standard ISO5832-12. Comparison of the phase compositions within group of ST_n, n=1,2,3,4 showed that the surface texturing had no significant effect to the phase constitution, whereas comparison between group ST and group PCST showed that it was significantly changed by the following LTPC process. Two strong peaks near 40° and 47° on the PCST samples can be indexed to S-phase S (111) and S-phase S (200). These two peaks were in position similar to α (111) and α (200) on UT samples but shift to the smaller angles. Quantitative calculation revealed that the d-spacing of S (111) on PC sample near 43° increased from 2.071 nm to 2.238 nm — sign of the super-saturation of atomic carbon in CoCrMo α -FCC phase.

3.2 Mechanical and tribological properties

3.2.1 Pendulum CoF and film thickness

The friction coefficients calculated from the pendulum simulator are displayed in figure 6. It can be seen that the surface covered with S-phase (PC) showed moderately higher friction coefficient ($\text{CoF}_{\text{PC}}=0.20-0.21$) compared to untreated CoCrMo heads ($\text{CoF}_{\text{UT}}=0.19$). This is probably a negative effect of the high carbon content in the surface to the friction coefficient, which has been reported previously by Luo et al. [22]. It also can be seen that the duplex treated metal femoral heads has lower friction than PC ($\text{CoF}_{\text{PCST}}=0.18-0.19$), indicating the effectiveness of texturing in reducing friction between bearings. Although the coefficient value for PCST samples showed inconsistency between variable types of

textures, the remarkable reduction can be found for samples textured with 9.5 μm sized dimples ($\text{CoF}_{\text{PCST4}}=0.15$ in average).

The hip joint simulator, employed in the present study, allowed investigating lubrication processes during swing motion in a range of -16° to 16° . Figure 7 compares the damping transient sinusoidal motion of tested femoral head when they wore against UHMWPE. At the marked test points, the film thickness were measured and interferometry image at the start, the middle and the end of damping are shown in figure 8, 9, and 10, respectively. At the start of motion, the film thickness of the UT sample was mostly restricted by the sliding speed, where the film thickness at equilibrium ($v_D=6$ mm/s, $u_D=150$ nm) was much higher than that of amplitudes ($v_A=0$ mm/s, $u_A=40$ nm). In comparison, the textured surface showed better lubrication status at the beginning of test (i.e. $v_D=6$ mm/s, $u_D=532$ nm), although it also followed the rule of film thickness being influenced by the relative sliding speed of bearings (i.e. $v_A=0$ mm/s, $u_A=25$ nm). At the middle of damping, the film thickness of UT was increased by a combination effect of the sliding speed and absorbed protein molecules. It is perhaps hard to predict which effect was predominant but the combination of both effects led to the relative thick film at both equilibrium and amplitude positions (i.e. $v_B=0$ mm/s, $u_B=100$ nm; $v_E=3.7$ mm/s, $u_E=100$ nm). As for the ST4 sample, the interferometry image at amplitude was very interesting, where the film thickness of the textured area on the left side ($v_B=0$ mm/s, $u_B=450$ nm) was higher than that of the non-textured area on the right side. Towards the end of damping, film thickness kept at 80 nm, regardless of the sliding speed being almost zero, indicating the establishment of aggregated protein film towards the end of test.

3.2.2 Dynamic friction coefficient

It is possible to determine the kinetic friction coefficient during cyclic start-and-stop sliding condition with the reciprocating tester. The typical friction coefficient of the untreated CoCrMo (UT) and surface textured CoCrMo (ST) under normal force is summarised in figure 11. It can be seen that the untreated CoCrMo surface exhibited a relatively unstable and fluctuating friction during stroke. At the beginning of

movement, the friction coefficient was high ($\text{CoF}_{\text{start}}=0.32$) when the pin started to move from velocity zero, but it quickly decreased to around 0.25 as the motion started. As for the dimpled surface, the friction coefficient line was flat throughout stroke of textured samples. As show in figure 11, average friction coefficients of different patterns were compared as follows:

$$\text{CoF}_{\text{ST4}} < \text{CoF}_{\text{ST1}} < \text{CoF}_{\text{ST2, ST3}} < \text{CoF}_{\text{UT}}$$

It is clear to see that the 9.5 μm sized dimples showed the lowest friction among all texted samples. The friction coefficient of all samples showed incremental increase after each stroke (figure 11b), e.g. from 0.15 to 0.16 and from 0.18 to 0.29 for PCST4 and UT, respectively.

3.2.3 Post-wear friction coefficient

There was a little abrasive wear found on metal untreated femoral head after wearing against UHMWPE, and long scratches with length of up to 6 mm can be visually seen over the contact area. In contrast, the PCST samples were very smooth with microscopic scale fine scratches. No severe damage of UHMWPE surface was observed after the wear test. It was difficult to obtain quantitative volume of the mild wear on MoP bearings. Therefore, after retrieved from ball-in-cup sliding wear, the friction coefficient of all samples was repeated on pendulum simulator. Results were shown as before and after wear test in figure 12. It can be seen that all samples showed increased friction coefficient after ball-in-cup wear. Friction coefficients in the beginning were 0.19 for UT, 0.18-0.19 for PCST1 & PCST2 & PCST3, and 0.15 for PCST4, and it increased to 0.3 for UT, 0.21 for PCST1,2 and 0.17 for PCST4 after ball-in-cup. The profilometer confirmed that the surface roughness R_a of CoCrMo surface increased from 0.15 μm to around 0.25 μm for UT (figure 12). Nano-hardness tests confirmed that the surface hardness was increased from 5 GPa for untreated surface to 16 GPa for LTTPC treated surfaces.

4 Discussion:

Wear of the prosthesis bearing surface under high load is an unavoidable process for artificial joint. Abrasive wear occurs when the bearing components enter in contact with the areas where the thickness of fluid lubricant film becomes very similar to the roughness of the articulating surfaces. In a study of wear investigation on revised metal-on-UHMWPE hip prosthesis, the average penetration depth is 0.20 mm/year and the wear volume rates is 55 mm³/year [31]. It is known that the dominant reason of revision was acetabular loosening, leading to revision rate of 25 % at only 20 years of service [32]. Surface with minimum material lose has been developed from different approaches in terms of MoP hip replacement materials, such as lowering the friction coefficient or increasing hardness of polymer liner. Polishing surface to its minimum surface roughness is one primary and useful way to lower the friction coefficient. However, it is very difficult, if not impossible, to maintain clean roughness at level of 0.01 at long-term conditions. It was reported that surface roughness of the implant metal head can increase from 0.01-0.02 μm to 0.06-0.19 μm after service [31, 33].

Surface texture has been reported can offers improvement on the lubrication properties by generating additional lubricant stored in cavities during sliding movement [18, 19]. Other benefits of surface texture in terms of decreasing adhesion and wear of components is related to its mechanisms of controlling flow of wear debris and decreasing contact area to reduce further wear, in particular, it sustains the fluid film by reducing third body abrasion [34]. However, the surface texture design for hip prosthesis is complicated, particularly for such conditions with low speed and high load as in mix to boundary lubrication. The previous mathematical models established to evaluate the hydrodynamic effect of dimples under ball-on-flat conditions might not be suitable for the analysing of hip prosthesis bearings. The pendulum testing of friction coefficient used in this study allows comparison between various modified materials surface and the untreated MoP hip prosthesis [35, 36]. This method has been improved by integrating the viscous damping to acquire higher accuracy of prediction of friction [27]. Our study

using this method to predict friction showed that the friction coefficient was reduced on ST4, and ST4 which were treated with micro-size dimples (figure 6). This result is in line with other studies where micro-sized texture with higher texture area density is possibly more beneficial for fluid flow control [34]. Although the lubricating mechanism existing within real replacement bearings is difficult to be measured, the technique used in this study is able to give some detailed information about the lubricant film distribution within the contact, and it is the only method one can provide up-to-date, proves that the film thickness increasing around textured area of prosthesis contact surface (figure 9). Our study also showed that the bovine serum solution as a tribologically tested lubricant has an impact to alter the friction coefficient during film thickness test and reciprocating CoF test in a short time (figure 11). This phenomenon of increasing in friction coefficient has been reported by Scholes et al. [37]. It was suggested that proteins present between the sliding surfaces might have effect to the friction coefficient. Sliding with BS solution creates a time-dependant film thickness characteristics due to the formation of a thin adherent film, which is believed formed by aggregation of absorbed protein molecules on the surface.

Dimple density, dimple width and depth, texture array and dimple shapes/orientation are major parameters for designing of texture patterns. For many research concerning the effect of those parameters, the results are inconclusive [38-41]. Studies showed that dimple density plays a vital role and it was suggested that 20 %-40 % of density can generate maximised hydrodynamic pressure. The depth-over-width ratio of dimples is another important parameter and it is preferred to be in the range of 0.01-0.05. The width of dimples also limits the number of dimples existing in the area of Hertz contact. The optimal values of parameters obtained in this study, however, do not entirely agree with the theoretical values. The best tribological performance is found on the PCST4, with 58% dimple density and 0.5 depth-over-width ratio. The shapes and array of dimples demonstrate no significant effect to the CoF of bearings. This is evidenced by comparing the CoF of ST2 and ST3 and their pattern parameters — two different arrays having similar CoF results. This is an indication of the importance of lubrication retaining effect of texture under conformal high speed low load conditions, rather than the hydrodynamic effect with

sensitivity to shallow and small shapes. Additionally, the higher film thickness of ST4 at the start of motion ($u=532$ nm, figure 8) and smaller friction coefficient found at the start of movement for all dimpled samples (figure 11b) indicated that the texture might decrease the initial static friction between bearings and probably prevent the stiction at low speed.

Since texture with the micrometre sizes are preferable to achieve effective level of friction reduction [42], the protection of such small texture from severe wear seems needed for long-term application. This study showed that for untreated femoral heads, constant low friction coefficient cannot be obtained under high-load wearing conditions (figure 12). This can be evidenced by the scratches on the CoCrMo femoral head, increase in friction coefficient after 16,560 wear cycles, and subsequent increasing of roughness (figure 12). In comparison, the friction coefficient found for PCST4 is significantly lower than the others. This improvement was probably attributed to the durability of relative large size dimples and the hardening thereof from LTPC process. The hardness of the duplex treatment on femoral head increasing from 5 GPa in the substrate to 16 GPa on the carburised surface plays an important role in reducing the abrasion damage of dimples during sliding wear [26, 43].

Unlike coatings, diffusion methods modify the chemical composition of the surface with atomic interstitial carbon, thus it can harden the substrate of component to a certain depth. Low temperature plasma carburising can eliminate the risk of delamination or surface cracking of thin film and coatings, which are the major concern of using coatings for orthopaedics. To sum up, the thermal chemical treatment is superior to coatings in the way that it doesn't cause third body wear due to the debonded particles. The duplex surface engineered system has combined benefit from both texturing and surface hardening. It lowers the friction between MoP pairings, reduce wear for both metal and polymer surfaces, and improves service life of UHWPE. Another advantage is that hardened surface reduces the release of metal particles and metal ions thus it reduces the risk of metal hypersensitivity. Although results from the ball-in-cup wear machine provide little reference for the quantitative measure of wear on the surface of hip joint, our comparative results shows that surface texture and low-temperature plasma carburising

duplex treatment on CoCrMo head could be a cost-effective approach to achieve practically durable low friction MoP bearing surface. However, the current preliminary study has been limited to the creation of texture on the metal surface. The effect of texture created on the polymer counterpart in the same measurement conditions, and whether the positive effect would be compromised by the wear of soft polymer material are worthy of investigation.

5 Conclusion

A low-cost surface engineering process that combines surface texturing and plasma surface engineering is developed to create a prototype surface for CoCrMo ISO 5832-12 on UHMWPE hip replacement. Surface texture with various geometric parameters is created on the femoral head and its wear property was tested against UHMWPE. Pendulum friction coefficient test showed that texture with micro-meter size can reduce the friction coefficient between head and cup for MoP hip joint. The roughening of metal surface and increasing in friction coefficient were significant on textured samples after long cycle ball-in-cup wear; however, this can be mitigated with subsequent plasma carburising process. Overall, the duplex surface shows significant improvement of both friction and durability, and thus it is closer to meet the integrity requirements of materials to be used in the MoP hip replacement bearings.

Acknowledgments

This work is an output of cooperation between Czech Science Foundation under project no.: 13-30879P and MEYS under the National Sustainability Programme I (Project LO1202), the project CZ.1.07/2.3.00/30.0005 – “Support for the creation of excellent interdisciplinary research teams at Brno University of Technology” and the project CEITEC-Central European Institute of Technology CZ.1.05/1.1.00/02.0068 financed by European Regional Development Fund.

References

- [1] J. L. Tipper, P. J. Firkins, A. A. Besong, P. S. M. Barbour, J. Nevelos, M. H. Stone, et al., "Characterisation of wear debris from UHMWPE on zirconia ceramic, metal-on-metal and alumina ceramic-on-ceramic hip prostheses generated in a physiological anatomical hip joint simulator," *Wear*, vol. 250, pp. 120-128, 10/ 2001.
- [2] P. J. Firkins, J. L. Tipper, E. Ingham, M. H. Stone, R. Farrar, and J. Fisher, "A novel low wearing differential hardness, ceramic-on-metal hip joint prosthesis," *J Biomech*, vol. 34, p. 8, 10/ 2001.
- [3] U. Holzwarth and G. Cotogno. (2012). Total hip arthroplasty : State of the art, prospects and challenges. Available: <http://publications.jrc.ec.europa.eu/repository/handle/JRC72428>
- [4] C. P. Case, "Chromosomal changes after surgery for joint replacement," *J Bone Joint Surg Br*, vol. 83, p. 3, 11/ 2001.
- [5] H. Ito, K. Kaneda, T. Yuhta, I. Nishimura, K. Yasuda, and T. Matsuno, "Reduction of polyethylene wear by concave dimples on the frictional surface in artificial hip joints," *J Arthroplasty*, vol. 15, pp. 332-338, 2000.
- [6] Metrology and properties of engineering surfaces: Springer Science & Business Media, 2001.
- [7] A. Chyr, M. Qiu, J. W. Speltz, R. L. Jacobsen, A. P. Sanders, and B. Raeymaekers, "A patterned microtexture to reduce friction and increase longevity of prosthetic hip joints," *Wear*, vol. 315, pp. 51-57, 7/ 2014.
- [8] H. Sawano, S. Warisawa, and S. Ishihara, "Study on long life of artificial joints by investigating optimal sliding surface geometry for improvement in wear resistance," *Precis Eng*, vol. 33, pp. 492-498, 2009.
- [9] L. Gao, P. Yang, I. Dymond, J. Fisher, and Z. Jin, "Effect of surface texturing on the elastohydrodynamic lubrication analysis of metal-on-metal hip implants," *Tribol Int*, vol. 43, pp. 1851-1860, 10/ 2010.
- [10] B. Zhang, W. Huang, J. Wang, and X. Wang, "Comparison of the effects of surface texture on the surfaces of steel and UHMWPE," *Tribol Int*, vol. 65, pp. 138-145, 2013.
- [11] D. Choudhury, F. Urban, M. Vrbka, M. Hartl, and I. Krupka, "A novel tribological study on DLC-coated micro-dimpled orthopedics implant interface," *J Mech Behav Biomed Mater*, vol. 45, pp. 121-131, 5/ 2015.
- [12] H. Yu, X. Wang, and F. Zhou, "Geometric shape effects of surface texture on the generation of hydrodynamic pressure between conformal contacting surfaces," *Tribol Lett*, vol. 37, pp. 123-130, 2010.
- [13] I. Krupka, P. Svoboda, and M. Hartl, "Effect of surface topography on mixed lubrication film formation during start up under rolling/sliding conditions," *Tribol Int*, vol. 43, pp. 1035-1042, 5/ 2010.
- [14] I. Krupka, M. Hartl, and P. Svoboda, "Effects of surface topography on lubrication film formation within elastohydrodynamic and mixed lubricated non-conformal contacts," *Proc Inst Mech Eng J*, vol. 224, pp. 713-722, 8/ 2010.
- [15] S. M. Hsu. (2006). Surface texturing: principles and design. Available: http://www.zdrax.de/en/assets/pdf/Surface_Texturing_Principles_and_Design.pdf
- [16] M. Vrbka, O. Šamánek, P. Šperka, T. Návrat, I. Křupka, and M. Hartl, "Effect of surface texturing on rolling contact fatigue within mixed lubricated non-conformal rolling/sliding contacts," *Tribol Int*, vol. 43, pp. 1457-1465, 8/ 2010.
- [17] M. Vrbka, I. Křupka, O. Šamánek, P. Svoboda, M. Vaverka, and M. Hartl, "Effect of surface texturing on lubrication film formation and rolling contact fatigue within mixed lubricated non-conformal contacts," *Meccanica*, vol. 46, pp. 491-498, 6/ 2011.

- [18] I. Křupka, R. Poliščuk, M. Vaverka, M. Hartl, M. Vrbka, and O. Šamánek, "Effect of surface texturing on lubrication film formation within non-conformal contacts," in *Advan Tribol*, J. Luo, Y. Meng, T. Shao, and Q. Zhao, Eds., ed: Springer Berlin Heidelberg, 2010, pp. 84-85.
- [19] I. Křupka and M. Hartl, "The effect of surface texturing on thin EHD lubrication films," *Tribol Int*, vol. 40, pp. 1100-1110, 7/ 2007.
- [20] T. Bell and Y. Sun, "Low-temperature plasma nitriding and carburising of austenitic stainless steels," *Heat Treat of Met*, vol. 29, pp. 57-64, 2002.
- [21] T. Bell and C. X. Li, "Stainless steel - Low temperature nitriding and carburizing," *Adv Mater Process*, vol. 160, pp. 49-51, 2002.
- [22] X. Luo and X. Li, "Design and characterisation of a new duplex surface system based on S-phase hardening and carbon-based coating for ASTM F1537 Co–Cr–Mo alloy," *Appl Surf Sci*, vol. 292, pp. 336-344, 2/ 2014.
- [23] X. Y. Li, N. Habibi, T. Bell, and H. Dong, "Microstructural characterisation of a plasma carburised low carbon CoCr alloy," *Surf Eng*, vol. 23, pp. 45-51, 2007.
- [24] H. Dong, "S-phase surface engineering of Fe-Cr, Co-Cr and Ni-Cr alloys," *Int Mater Rev*, vol. 55, pp. 65-98.
- [25] Y. Dong, X. Li, L. Tian, T. Bell, R. L. Sammons, and H. Dong, "Towards long-lasting antibacterial stainless steel surfaces by combining double glow plasma silvering with active screen plasma nitriding," *Acta Biomater*, vol. 7, pp. 447-57, 2011.
- [26] Y. Dong, X. Li, R. Sammons, and H. Dong, "The generation of wear-resistant antimicrobial stainless steel surfaces by active screen plasma alloying with N and nanocrystalline Ag," *J Biomed Mater Res B Appl Biomater*, vol. 93B, pp. 185-193, 2010.
- [27] J. J. Crisco, J. Blume, E. Teeple, B. C. Fleming, and G. D. Jay, "Assuming exponential decay by incorporating viscous damping improves the prediction of the coefficient of friction in pendulum tests of whole articular joints," *Proc Inst Mech Eng H*, vol. 221, pp. 325-33, 4/ 2007.
- [28] M. Vrbka, D. Nečas, M. Hartl, I. Křupka, F. Urban, and J. Gallo, "Visualization of lubricating films between artificial head and cup with respect to real geometry," *Biotribol*, vol. 1–2, pp. 61-65, 3/ 2015.
- [29] S. Corujeira Gallo, "Active screen plasma surface engineering of austenitic stainless steel for enhanced tribological and corrosion properties," Doctor of Philosophy, Department of Metallurgy and Materials, University of Birmingham, Birmingham, 2008.
- [30] J. Buhagiar and H. Dong, "S-Phase in stainless steels: An Overview," presented at the Surface modification technologies XXI, Ohio, 2007.
- [31] R. M. Hall, A. Unsworth, P. Siney, and B. M. Wroblewski, "Wear in retrieved charnley acetabular sockets," *Proc Inst Mech Eng H*, vol. 210, pp. 197-207, 9/ 1996.
- [32] H. Malchau, P. Herberts, T. Eisler, G. Garellick, and P. Soderman, "The Swedish Total Hip Replacement Register," *J Bone Joint Surg Am*, vol. 84-A Suppl 2, pp. 2-20, 2002.
- [33] A. W. Eberhardt, R. T. McKee, J. M. Cuckler, D. W. Peterson, P. R. Beck, and J. E. Lemons, "Surface Roughness of CoCr and ZrO₂ Femoral Heads with Metal Transfer: A Retrieval and Wear Simulator Study," *Int J Biomat*, vol. 2009, p. 1, 2009.
- [34] X. Wang, J. Wang, B. Zhang, and W. Huang, "Design principles for the area density of dimple patterns," *Proc Inst Mech Eng J*, 5/ 2014.
- [35] C. Brockett, S. Williams, Z. Jin, G. Isaac, and J. Fisher, "Friction of total hip replacements with different bearings and loading conditions," *J Biomed Mater Res B Appl Biomater*, vol. 81B, pp. 508-515, 2007.
- [36] M. P. Gispert, A. P. Serro, R. Colaço, and B. Saramago, "Friction and wear mechanisms in hip prosthesis: Comparison of joint materials behaviour in several lubricants," *Wear*, vol. 260, pp. 149-158, 1/ 2006.
- [37] S. C. Scholes and A. Unsworth, "The effects of proteins on the friction and lubrication of artificial joints," *Proc Inst Mech Eng H*, vol. 220, pp. 687-93, 2006.

- [38] G. C. Buscaglia, I. Ciuperca, and M. Jai, "On the optimization of surface textures for lubricated contacts," *J. Math. Anal. Appl.*, vol. 335, pp. 1309-1327, 11/ 2007.
- [39] X. Zhou, A. L. Galvin, Z. Jin, X. Yan, and J. Fisher, "The influence of concave dimples on the wear of ultra-high molecular weight polyethylene," *Proc Inst Mech Eng J*, vol. 226, pp. 455-462, 2012.
- [40] Y. Qiu and M. M. Khonsari, "Experimental investigation of tribological performance of laser textured stainless steel rings," *Tribol Int*, vol. 44, pp. 635-644, 5/ 2011.
- [41] J. Larsen-Basse, L. Ives, and S. M. Hsu, "Boundary lubricated friction experiments with coarse surface texture," presented at the ASME/STLE 2007 International Joint Tribology Conference, San Diego, California, USA, 2007.
- [42] H. Yu, W. Huang, and X. Wang, "Dimple patterns design for different circumstances," *Lubrication Science*, vol. 25, pp. 67-78, 2013.
- [43] T. Bell, "Surface engineering of steel to combat wear," *Metallurgica*, vol. 49, pp. 103-108, 1982.

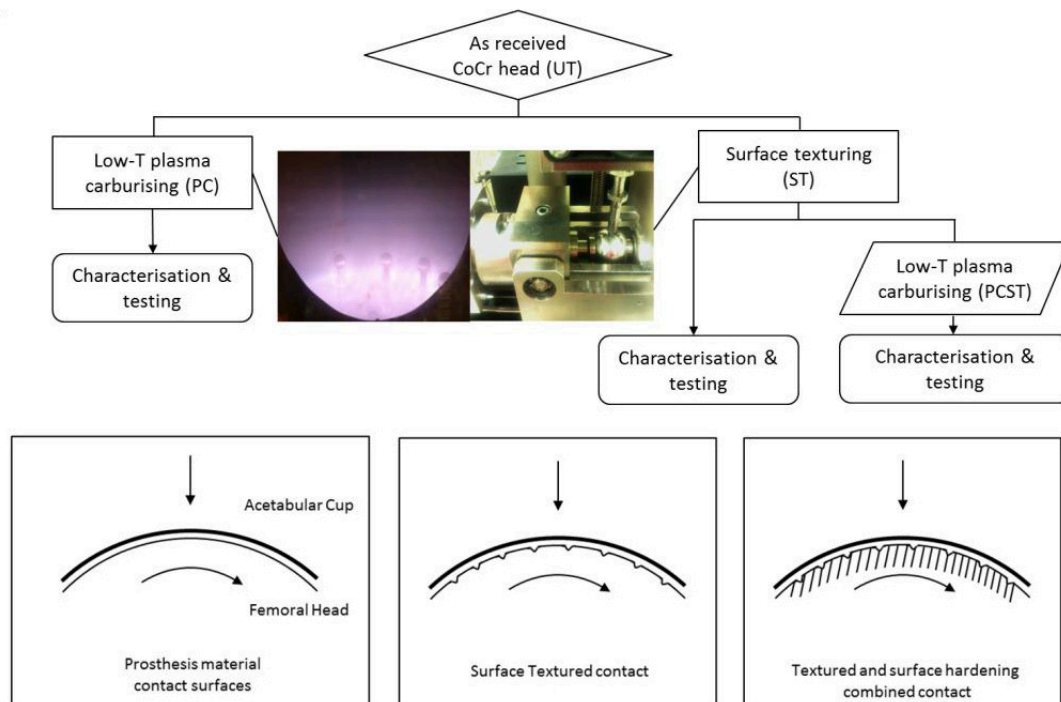


Figure 1 Experiment process flow chat (top), treatments photo (top-middle) and the illustrated hip replacement surface after the corresponding treatment (bottom)

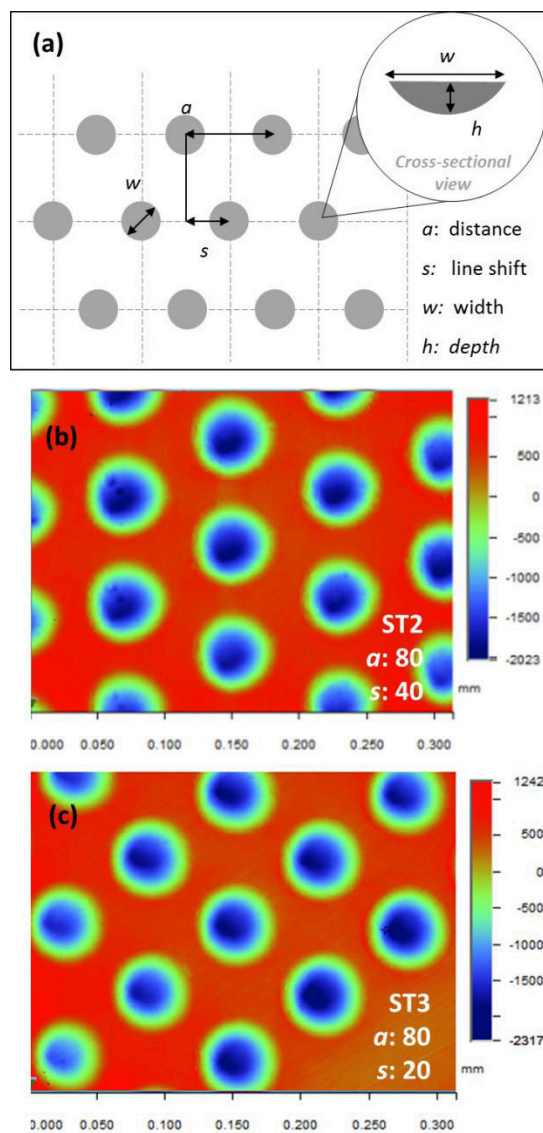


Figure 2 The pattern configurations (a) and 3-D optical profiles of two surface textured patterns with two line shifts

A

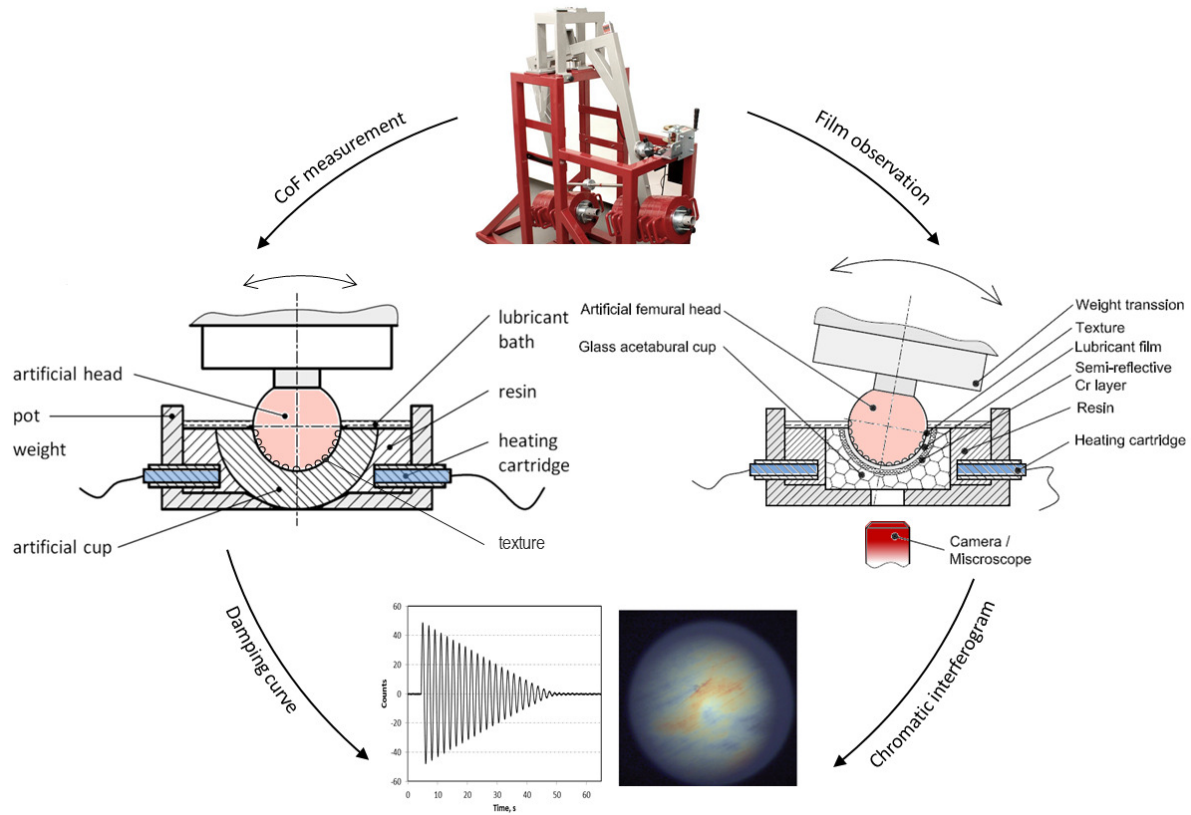


Figure 3 The hip replacement pendulum apparatus used for friction coefficient measurement and observation of lubricant film using optical test device

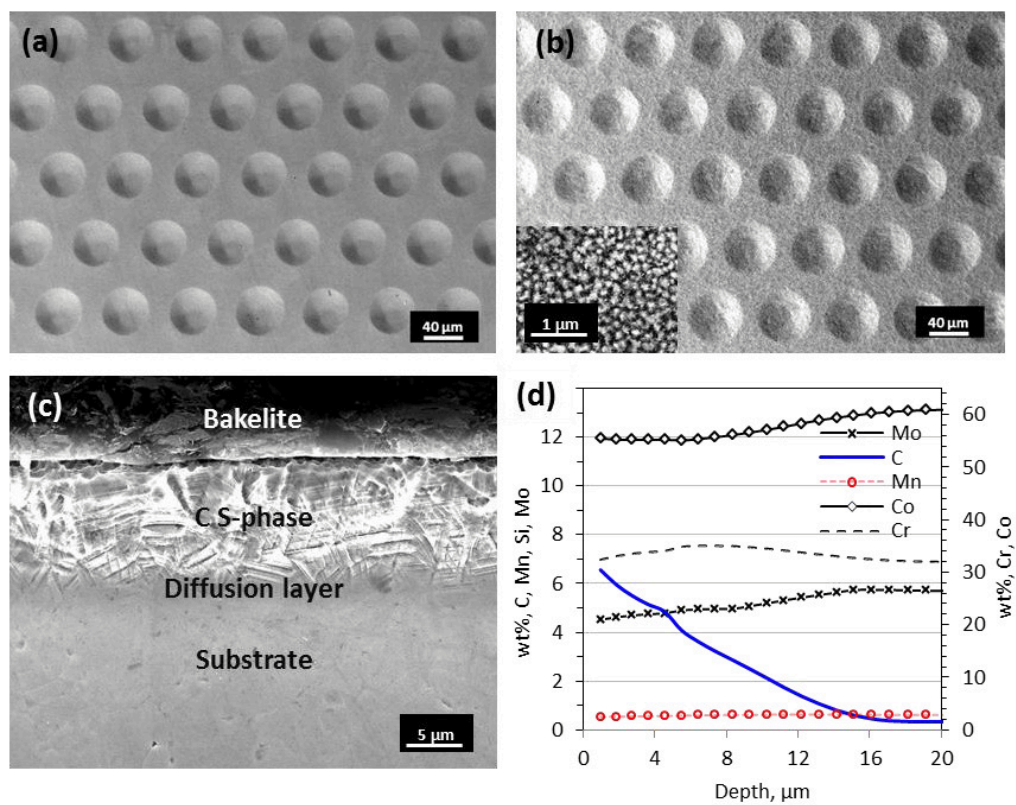


Figure 4 SEM images of (a) ST surface, (b) PCST surface (c) cross-sectional metallography, and (d) GDOES profile of PCST

Accepted

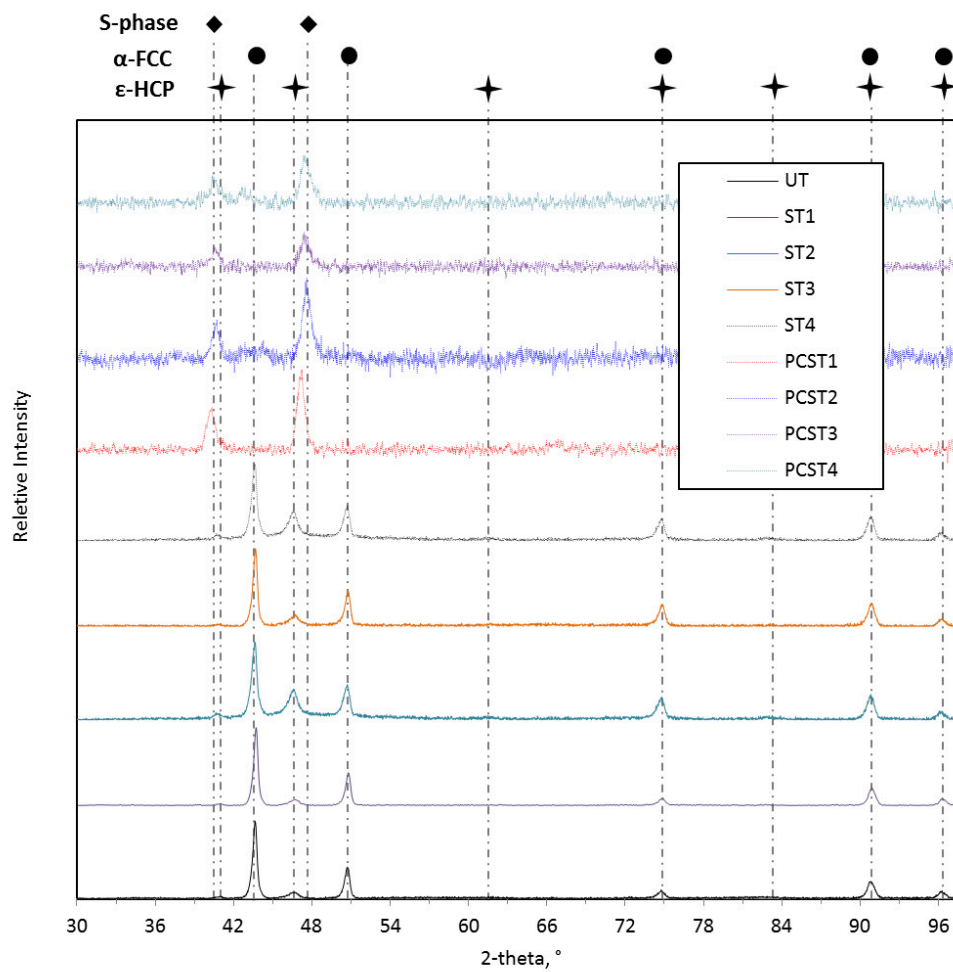


Figure 5 The XRD crystallography and the phase analysis

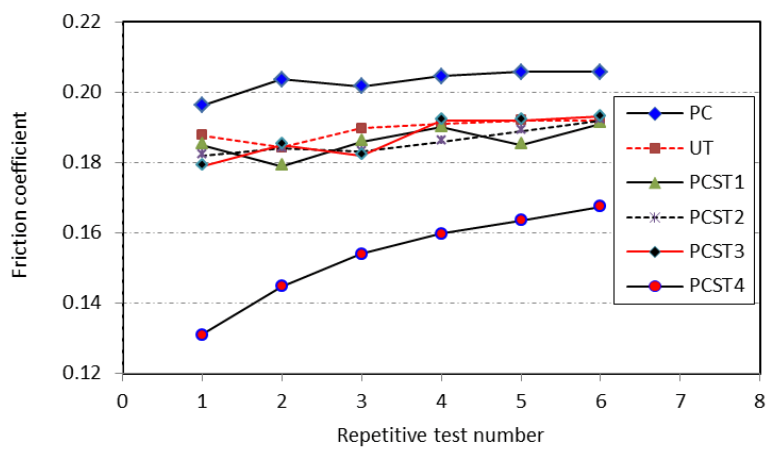


Figure 6 The friction coefficients of untreated and treated samples

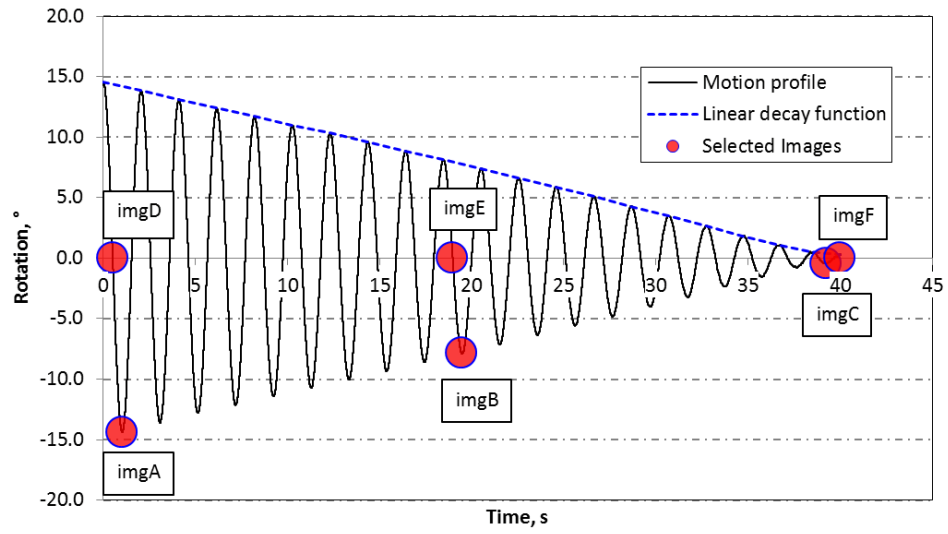


Figure 7 The damping curve measured by pendulum hip joint simulator and the selected points of interferometry

images

Accepted m

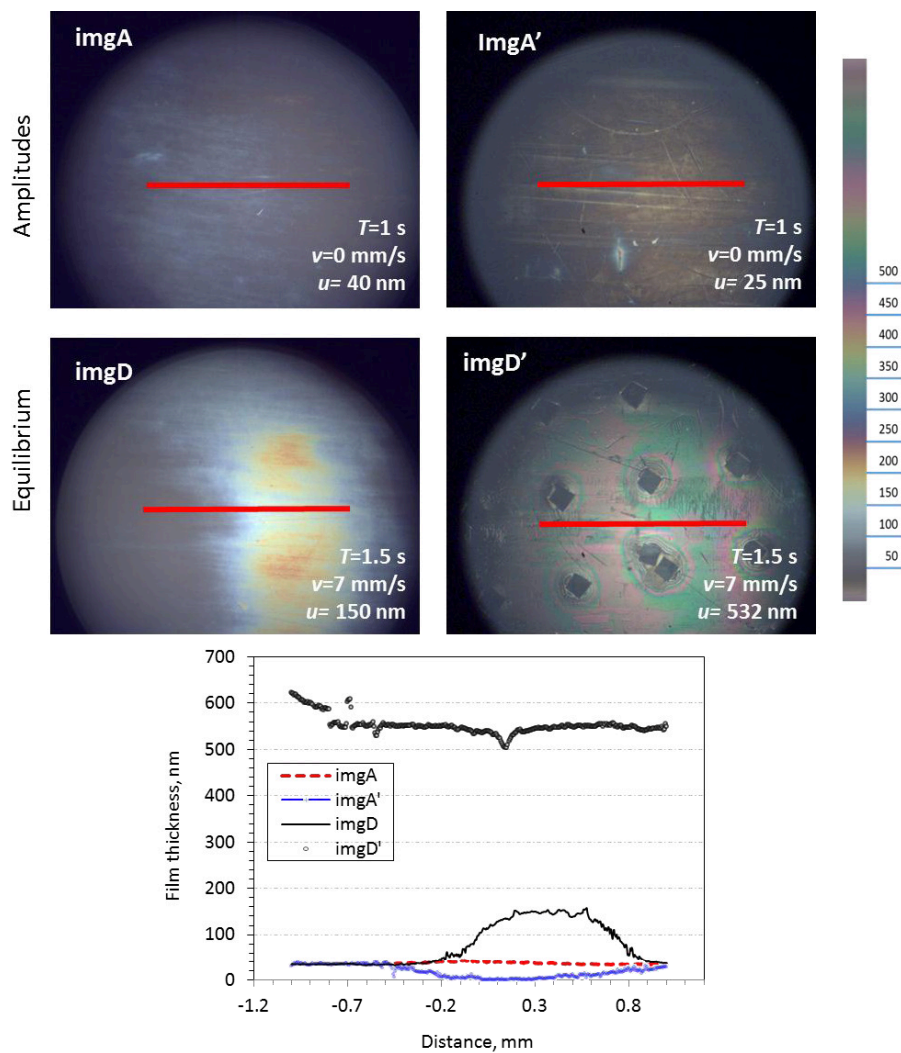


Figure 8 Chromatic interferograms of UT (imgA and imgD) and PCST4 (imgA' and imgD') at the beginning of pendulum oscillation, showing the lubricant film thickness (u , nm) in relation to time (T , s) and relative speed (v , mm/s) and the line profiles of film thickness at selected points

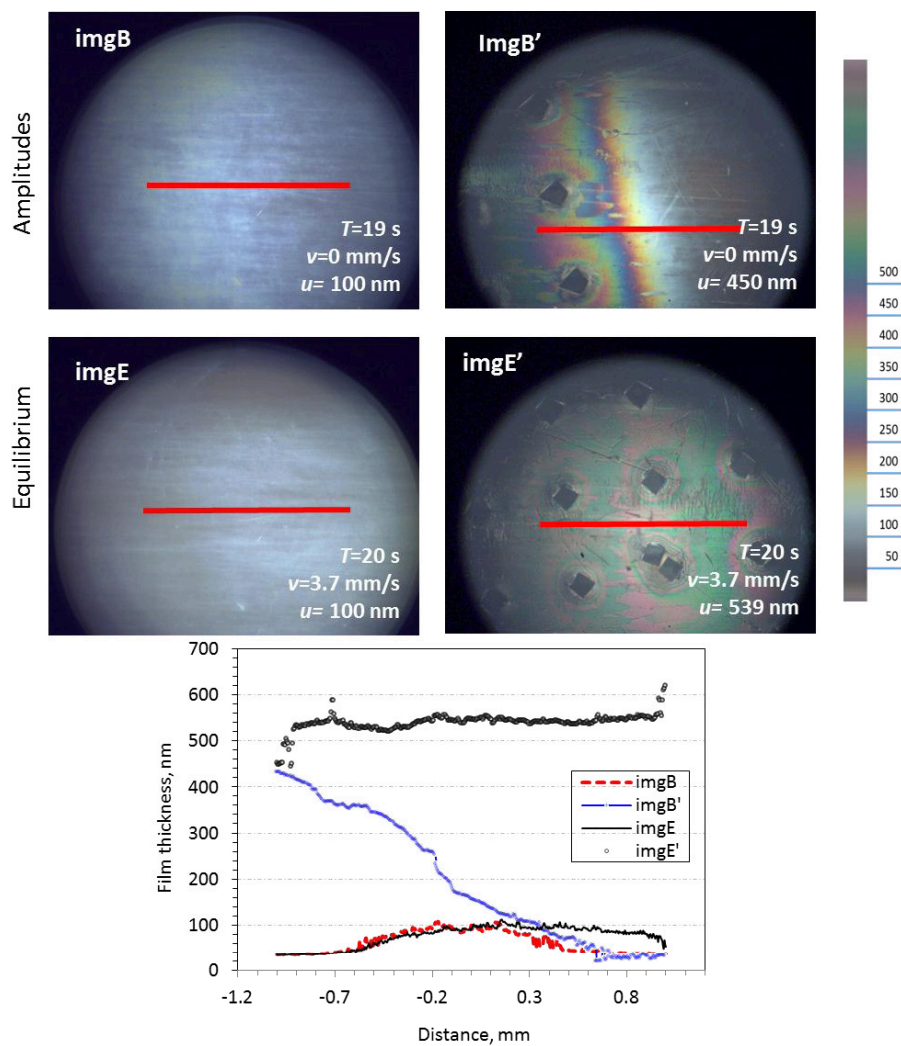


Figure 9 Chromatic interferograms of UT (imgB and imgE) and PCST4 (imgB' and imgE') at the middle of pendulum oscillation, showing the lubricant film thickness (u , nm) in relation to time (T , s) and relative speed (v , mm/s) and the line profiles of film thickness at selected points

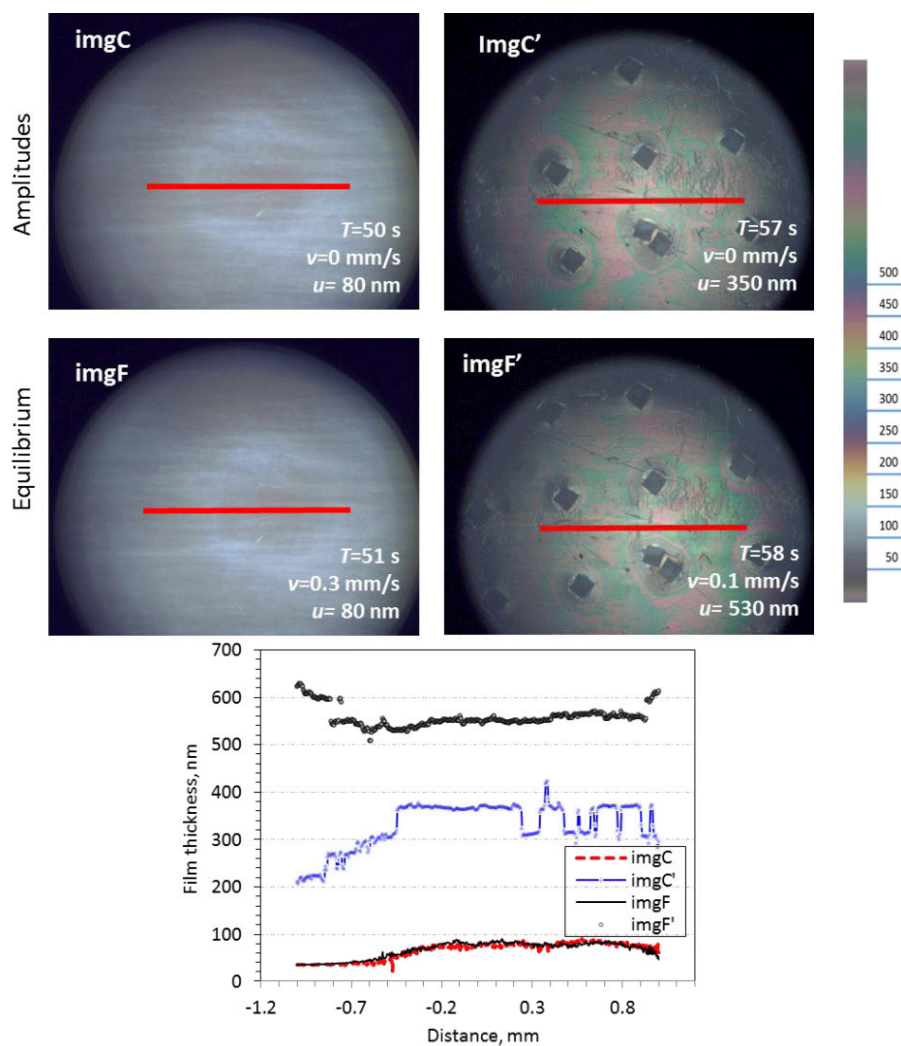


Figure 10 Chromatic interferograms of UT (imgC and imgF) and PCST4 (imgC' and imgF') at the end of pendulum oscillation, showing the lubricant film thickness (u , nm) in relation to time (T , s) and relative speed (v , mm/s) and the line profiles of film thickness at selected points

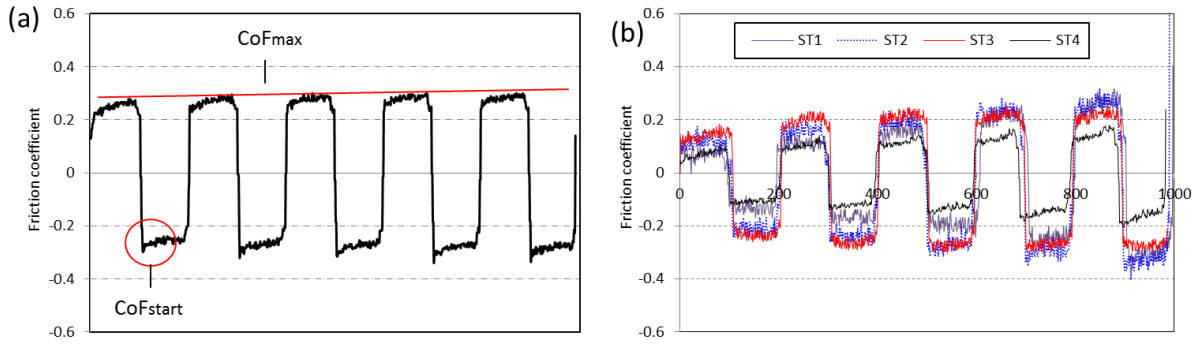


Figure 11 Reciprocating CoF profiles of (a) UT, and (b) PCST1, PCST2, PCST3 and PCST4

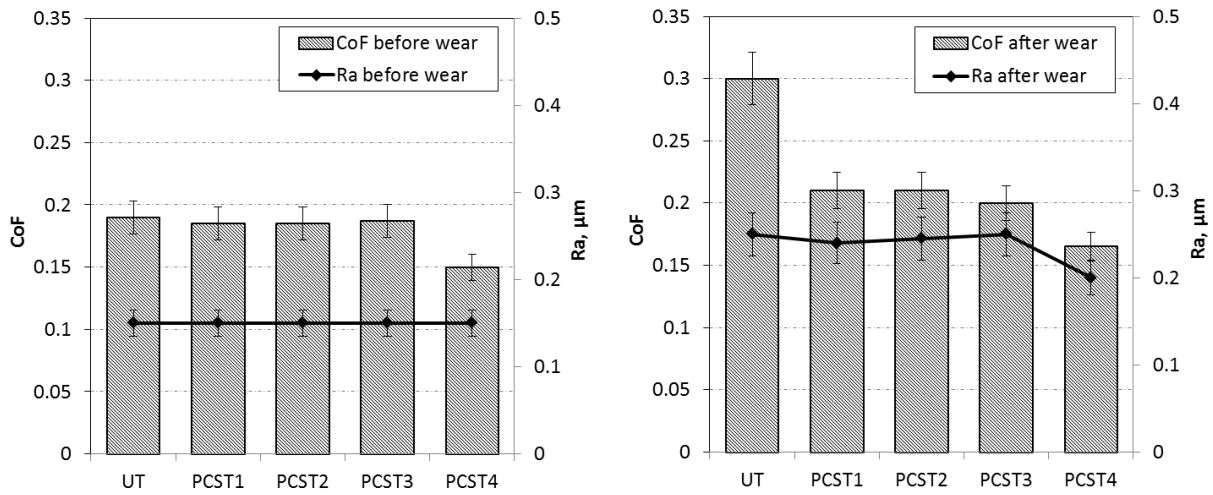


Figure 12 Friction coefficients and surface roughness of UT and PCST measured before and after wear

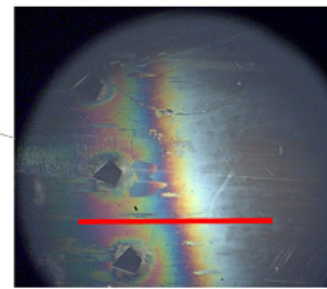
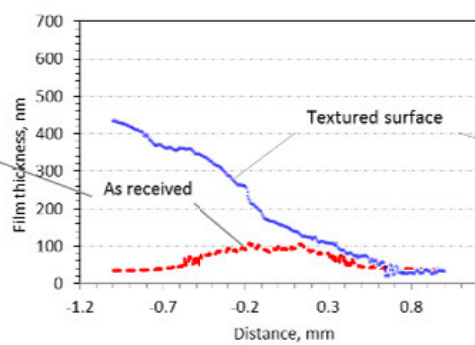
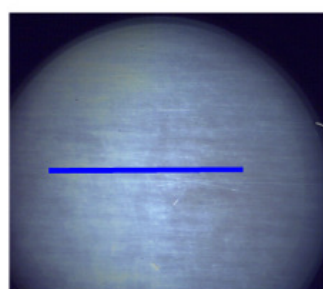
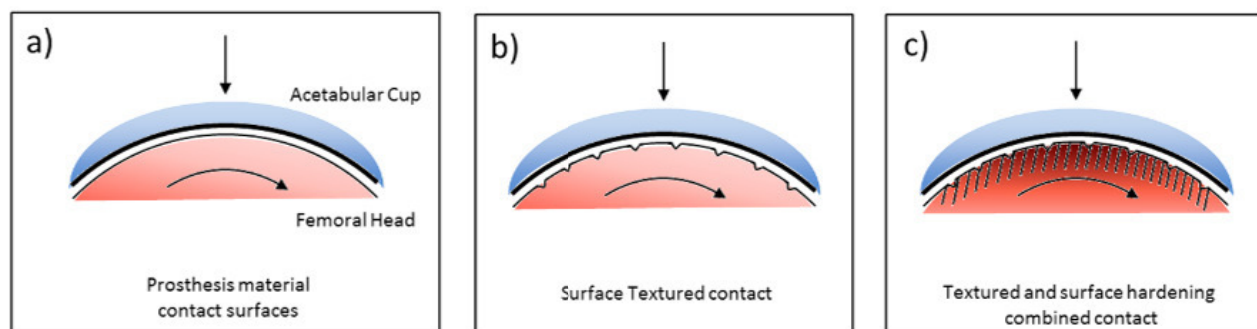
Table 1 The experimental parameters and the corresponding sample codes

Sample codes	Surface texturing	Sample codes after plasma carburising

	Depth h, μm	Width w, μm	Shape	s/a x100%	Distance a, μm	Dimple density %	
UT	-	-	-	-	-	-	PC
ST1	1.5	55	○	50%	80	37	PCST1
ST2	2.4	65	○	50%	80	52	PCST2
ST3	2.4	65	○	25%	80		PCST3
ST4	9.5	190	◇	0	500	58	PCST4

Highlights:

- An innovative duplex surface treatment (micro-texturing and S-phase) was developed.
- In-situ visualization of lubricating films on real geometry head and cup.
- Lubricating film thickness was increased by surface texturing on CoCrMo head.
- Testing time-dependant performance of dimpled surface and its longevity.
- Study of frictional behaviour of MoP joints with different texture geometries.



ACCEPTED MANUSCRIPT